

UCLA

UCLA Previously Published Works

Title

Quantitative Image Analysis at Chronic Lung Allograft Dysfunction Onset Predicts Mortality

Permalink

<https://escholarship.org/uc/item/9z79s20n>

Journal

Transplantation, 106(6)

ISSN

0041-1337

Authors

Weigt, S Samuel
Kim, Grace-Hyun J
Jones, Heather D
[et al.](#)

Publication Date

2022-06-01

DOI

10.1097/tp.0000000000003950

Peer reviewed

OPEN

Quantitative Image Analysis at Chronic Lung Allograft Dysfunction Onset Predicts Mortality

S. Samuel Weigt, MD, MS,¹ Grace-Hyun J. Kim, PhD,² Heather D. Jones, MD,³ Allison L. Ramsey, MD,¹ Olawale Amubieya, MD,¹ Fereidoun Abtin, MD,² Lila Pourzand, MD,² Jihey Lee, PhD,² Michael Y. Shino, MD, MS,¹ Ariss DerHovanesian, MD, MS,¹ Barry Stripp, PhD,³ Paul W. Noble, MD,³ David M. Sayah MD, PhD,¹ Rajan Saggari, MD,¹ Ian Britton, MD,¹ Joseph P. Lynch III, MD,¹ John A. Belperio, MD,¹ and Jonathan Goldin, MD, PhD²

Background. Chronic lung allograft dysfunction (CLAD) phenotype determines prognosis and may have therapeutic implications. Despite the clarity achieved by recent consensus statement definitions, their reliance on radiologic interpretation introduces subjectivity. The Center for Computer Vision and Imaging Biomarkers at the University of California, Los Angeles (UCLA) has established protocols for chest high-resolution computed tomography (HRCT)-based computer-aided quantification of both interstitial disease and air-trapping. We applied quantitative image analysis (QIA) at CLAD onset to demonstrate radiographic phenotypes with clinical implications. **Methods.** We studied 47 first bilateral lung transplant recipients at UCLA with chest HRCT performed within 90 d of CLAD onset and 47 no-CLAD control HRCTs. QIA determined the proportion of lung volume affected by interstitial disease and air-trapping in total lung capacity and residual volume images, respectively. We compared QIA scores between no-CLAD and CLAD, and between phenotypes. We also assigned radiographic phenotypes based solely on QIA, and compared their survival outcomes. **Results.** CLAD onset HRCTs had more lung affected by the interstitial disease ($P = 0.003$) than no-CLAD controls. Bronchiolitis obliterans syndrome (BOS) cases had lower scores for interstitial disease as compared with probable restrictive allograft syndrome (RAS) ($P < 0.0001$) and mixed CLAD ($P = 0.02$) phenotypes. BOS cases had more air-trapping than probable RAS ($P < 0.0001$). Among phenotypes assigned by QIA, the relative risk of death was greatest for mixed (relative risk [RR] 11.81), followed by RAS (RR 6.27) and BOS (RR 3.15). **Conclusions.** Chest HRCT QIA at CLAD onset appears promising as a method for precise determination of CLAD phenotypes with survival implications.

(*Transplantation* 2022;106: 1253–1261)

Chronic lung allograft dysfunction (CLAD) is the leading cause of morbidity and mortality beyond the first year post-lung transplantation,¹ but the course of disease is heterogeneous. It is increasingly recognized that CLAD phenotypes determine, at least in part, the prognosis after CLAD onset,^{1–7} but definitions and our understanding of CLAD phenotypes are evolving. In 2019, the International Society of Heart and Lung Transplantation (ISHLT) formalized definitions for CLAD and CLAD phenotypes in 2 consensus statements.^{6,7} CLAD is a persistent decline in forced expiratory volume in 1 second (FEV_1) of 20% or more from the post-transplant baseline.

CLAD can present as obstructive, restrictive, or mixed obstructive/restrictive phenotypes. The diagnosis of restrictive CLAD, officially termed restrictive allograft syndrome (RAS), is defined as CLAD with both a concomitant $\geq 10\%$ decline in total lung capacity (TLC) from the post-transplant baseline and persistent pulmonary opacities on chest imaging. Obstructive CLAD, still termed bronchiolitis obliterans syndrome (BOS), is defined as CLAD with associated indices of airflow limitation and without radiographic pulmonary opacities. Mixed CLAD is defined by physiologic restriction, airflow limitation, and persistent radiographic pulmonary opacities. CLAD with other

Received 30 March 2021. Revision received 28 July 2021.

Accepted 17 August 2021.

¹ Department of Medicine, University of California Los Angeles, Los Angeles, CA.

² Department of Radiology, University of California Los Angeles, Los Angeles, CA.

³ Department of Medicine, Cedars Sinai Medical Center, Los Angeles, CA.

All authors contributed to the design of the study. S.S.W., A.L.R., M.Y.S., A.D., P.W.N., D.S., R.S., J.P.L., and J.A.B. contributed to the acquisition of the data. S.S.W., G.J.K., H.D.J., L.P., J.L., and J.G. contributed to the development of the analysis plan. S.S.W., H.D.J., and J.L. performed the data analysis. All authors contributed to the interpretation of the data. S.S.W. and J.A.B. drafted the article. All authors critically revised the article and approved the final version for submission.

G.J.K. has an issued patent on quantitative imaging biomarkers in ILD (US-2015-0324982-A1) and received consulting fees from MedQIA, LLC. J.G. is the Founder of MedQIA, LLC. The other authors declare no conflicts of interest.

This research was supported by the NIH National Center for Advancing Translational Science (NCATS) UCLA CTSI Grant Number UL1TR001881 as well as the National Heart, Lung, and Blood Institute (NHLBI) Grant Number P01HL108793.

Correspondence: S. Sam Weigt, Department of Medicine, University of California Los Angeles Med-Pul & Critical Care; BOX 951690, 43-229 CHS; Los Angeles, CA 1690, (sweigt@mednet.ucla.edu).

Copyright © 2021 The Author(s). Published by Wolters Kluwer Health, Inc. This is an open-access article distributed under the terms of the Creative Commons Attribution-Non Commercial-No Derivatives License 4.0 (CCBY-NC-ND), where it is permissible to download and share the work provided it is properly cited. The work cannot be changed in any way or used commercially without permission from the journal.

ISSN: 0041-1337/20/1066-1253

DOI: 10.1097/TP.00000000000003950

combinations of restriction, obstruction, and pulmonary opacities are considered to have an undefined phenotype. These consensus definitions have since been validated in a single-center study where the BOS phenotype exhibited better post-CLAD survival than RAS or mixed CLAD.⁸

Despite the improvement in clarity achieved by the consensus statements, several aspects limit uniform application in practice. First, measurement of post-transplant TLC is not routinely performed in many transplant centers. In the absence of TLC measurements to define restriction, forced vital capacity (FVC) loss of $\geq 20\%$ from the post-transplant baseline can be used to imply restriction and meet criteria for “probable” RAS.^{6,7} However, FVC loss can also occur with air-trapping and hyperinflation, which are hallmarks of severe obstruction. Persistent radiographic pulmonary opacities support classification as RAS, but determination is subjective. In other instances, RAS might be present without meeting the FVC loss threshold at CLAD onset. Probable RAS was not examined in the previously mentioned CLAD definition validation study.⁸ Previously, we showed that the presence of parenchymal opacities at CLAD onset, even in the absence of FVC loss $\geq 20\%$, was sufficient to identify patients with a worse prognosis, implying RAS.² RAS like opacities also portend worse survival in patients with an undefined CLAD phenotype.⁸ The second source of uncertainty is the requirement for airflow limitation to diagnose BOS. The consensus suggests an $FEV_1/FVC < 0.7$ can indicate airflow limitation. However, data supporting the utility for $FEV_1/FVC < 0.7$ to define obstruction after lung transplantation are lacking. High-resolution computed tomography (HRCT) with end-expiratory images at residual volume (RV) can identify air-trapping.⁹ However, radiographic air-trapping was not included in criteria to define BOS.

Quantitative chest CT may also provide prognostic information in patients diagnosed with CLAD.¹⁰ The Center for Computer Vision and Imaging Biomarkers at the University of California, Los Angeles (UCLA) has established protocols for HRCT-based computer-aided

quantification of both interstitial lung disease and air-trapping. In this study, we applied quantitative image analysis (QIA) to chest HRCT at CLAD onset to demonstrate radiographic phenotypes with clinical implications.

MATERIALS AND METHODS

Study Cohorts

We conducted a retrospective study of first bilateral lung transplant recipients at UCLA between July 1, 2005 and June 30, 2014 ($n = 194$) (UCLA IRB# 18-000355). Data were collected through December 31, 2018. CLAD was defined as a sustained $\geq 20\%$ decline in FEV_1 as compared with the average of the 2 best post-transplant FEV_1 measured at least 3 wk apart in the absence of other clinical confounders.⁷ Patients with CLAD ($n = 72$) who had undergone standard of care noncontrast volumetric thin section chest CT within 90 d from CLAD onset ($n = 54$ CLAD) were eligible for inclusion. We excluded 7 potential CLAD cases because of conditions that confounded QIA (Figure 1), leaving 47 eligible CLAD onset CT scans. We also identified 47 no-CLAD controls with CT scans performed in stable bilateral lung recipients at similar durations post-transplant (Figure 1).

All patients received standardized immunosuppression, pulmonary function test follow-up, surveillance bronchoscopies, and other clinical management as previously described.¹¹ Treatment of CLAD was not standardized and differed on a case-by-case basis. However, macrolide therapy was routinely included for the treatment of CLAD. The study was approved by the UCLA Institutional review board (10-001492).

CLAD Phenotype Determination

CLAD phenotypes were determined according to ISHLT consensus definitions,^{6,7} with the following modifications. Restriction was inferred from FVC loss of $\geq 20\%$ from the post-transplant baseline at CLAD onset, thus classification as “probable” RAS when present in combination with

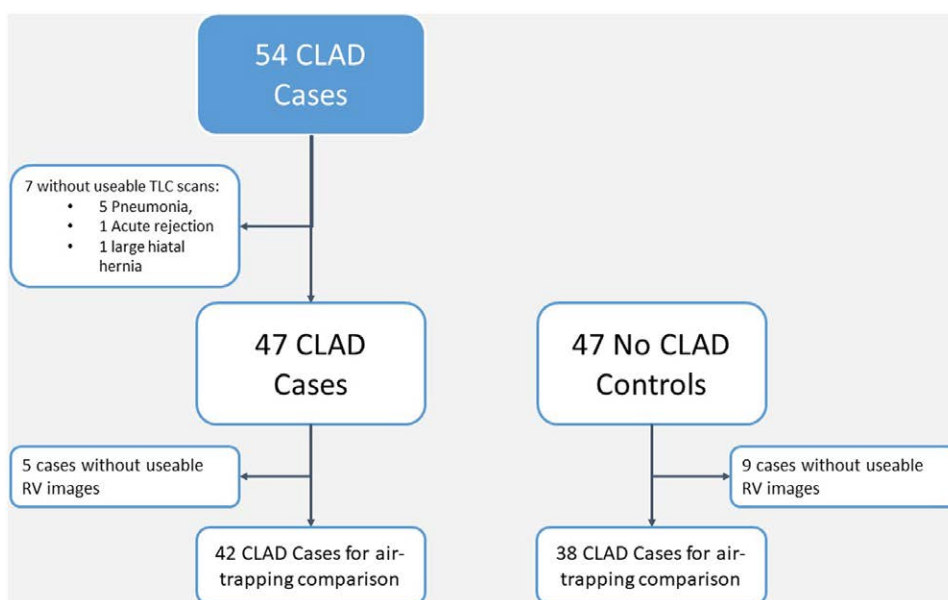


FIGURE 1. Selection of CLAD cases and no-CLAD controls. CLAD, chronic lung allograft dysfunction; TLC, total lung volume; RV, residual volume.

persistent pulmonary infiltrates and no airflow obstruction. Airflow obstruction was inferred by $FEV_1/FVC < 0.7$, and when present in the absence of FVC loss and without pulmonary infiltrates, subjects were classified as BOS. The presence of persistent pulmonary infiltrates was abstracted from clinical radiology reports. When both restriction and obstruction were inferred simultaneously by pulmonary function (eg, FEV_1 loss $\geq 20\%$, FVC loss of $\geq 20\%$, and $FEV_1/FVC < 0.7$), subjects were classified as BOS in the absence of pulmonary infiltrates, and as mixed CLAD in the presence of persistent pulmonary infiltrates. All other combinations of restriction, obstruction, and pulmonary infiltrates were classified as undefined CLAD.

Computer-aided Quantification of Interstitial Disease and Air-trapping

QIA of the lung parenchyma on TLC scans was performed using a previously published in-house algorithm scoring as a percentage the extent of quantitation of ground glass (QGG), quantitation of lung fibrosis (QLF), and quantitation of honeycombing (QHC).^{12,13} Total quantitation of interstitial lung disease (QILD) represents the sum of QHC + QLF + QGG. Quantitative air-trapping scores from end-expiration or RV HRCT images were calculated as percents of voxels below -856 hounsfield units from the histogram of segmented lung.

Statistical Methods

Demographic and baseline characteristics were summarized using descriptive statistics. Continuous variables were summarized as median and interquartile range (IQR). Categorical variables were summarized using counts and percentages. Nonparametric Wilcoxon *t* tests (2-tailed *P*) were used to assess differences for demographic and baseline characteristics across groups, and Fisher exact tests were used to evaluate frequency differences. QIA scores for interstitial disease (QILD, QLF, and QGG) and for air-trapping were compared using Kruskal-Wallis and post hoc Dunn tests. Overall survival and freedom from retransplant or death were estimated using the Kaplan-Meier method. We constructed a Cox proportional hazards model to assess for an association between CLAD phenotypes and post-CLAD mortality. Statistics were performed in GraphPad Prism 6 or JMP Pro 15.

RESULTS

Subject Characteristics

Of the 54 potential cases identified based on HRCT performed within 90 d of CLAD onset, we excluded 7 for conditions that confounded QIA; 5 for suspected pneumonia, 1 for acute rejection, and 1 for a large hiatal hernia causing atelectasis (Figure 1). Of the 47 eligible CLAD cases, 42 had adequate expiratory images for air-trapping assessments. For the 47 no-CLAD controls, 38 had adequate expiratory images. The characteristics of CLAD cases and no-CLAD controls are shown in Table 1. Subjects in each cohort were generally similar without significant differences.

Quantitative Image Analysis for CLAD Onset Cases and No-CLAD Controls

The proportion of lung affected by honeycomb changes was very low and not different between CLAD onset and

TABLE 1.
Subject characteristics

	Controls	CLAD	<i>P</i>
Sex, n (%)			0.14
Male	23 (49)	31 (66)	
Female	24 (51)	16 (44)	
Age at transplant, y	56 (47–59)	54 (42–60)	0.85
Race, n (%)			0.13
White	36 (77)	32 (68)	
Black	5 (11)	2 (4)	
Other	6 (13)	13 (28)	
Pretransplant diagnosis group, n (%)			0.77
A (obstructive lung disease)	13 (28)	10 (21)	
B (pulmonary vascular disease)	3 (6)	5 (11)	
C (cystic fibrosis)	5 (11)	7 (15)	
D (restrictive lung disease)	26 (55)	25 (53)	
Days posttransplant to CT chest	743 (546–1373)	838 (549–1517)	0.45

CLAD, chronic lung allograft dysfunction; CT, computed tomography.

no-CLAD control HRCTs. However, CLAD onset HRCTs had significantly more lung affected by QLF, QGG, and total QILD (Table 2 and Figure 2).

The proportion of lung volume affected by air-trapping in CLAD onset HRCTs was 9.3% (IQR 1.6–24.1%), as compared with 5.1% (IQR 1.6–12.1%) in no-CLAD controls, which was not statistically significant (*P* = 0.18) (Figure 3).

Quantitative Image Analysis for CLAD Phenotypes

We classified CLAD cases as BOS, probable RAS, mixed CLAD, or undefined CLAD based on 2019 ISHLT consensus definitions for CLAD phenotypes. Among our 47 cases, we classified 15 BOS, 13 probable RAS, 4 mixed CLAD, and 15 undefined CLAD phenotypes. We compared HRCT scores for interstitial disease and its components, as well as for air-trapping, between CLAD phenotypes (Figure 4). BOS cases had significantly lower scores for QGG and total QILD, as compared with probable RAS, mixed, and

TABLE 2.
Chest HRCT QIA Scores for ILD components and total ILD

	Controls	CLAD	<i>P</i>
Quantitation of honeycombing (QHC)	0.1% (0.1–0.2)	0.1% (0.1–0.3)	0.19
Quantitation of lung fibrosis (QLF)	0.8% (0.5–1.7)	1.5% (0.6–4.8)	0.005
Quantitation of ground glass (QGG)	5.0% (2.9–7.1)	9.4% (3.7–19.2)	0.004
Total ILD (QILD)	5.9% (3.6–8.3)	10.8% (4.4–21.7)	0.003

CLAD, chronic lung allograft dysfunction; HRCT, high-resolution computed tomography; QHC, quantitation of honeycombing; QLF, quantitation of lung fibrosis; QGG, quantitation of ground glass; QILD, quantitation of interstitial lung disease.

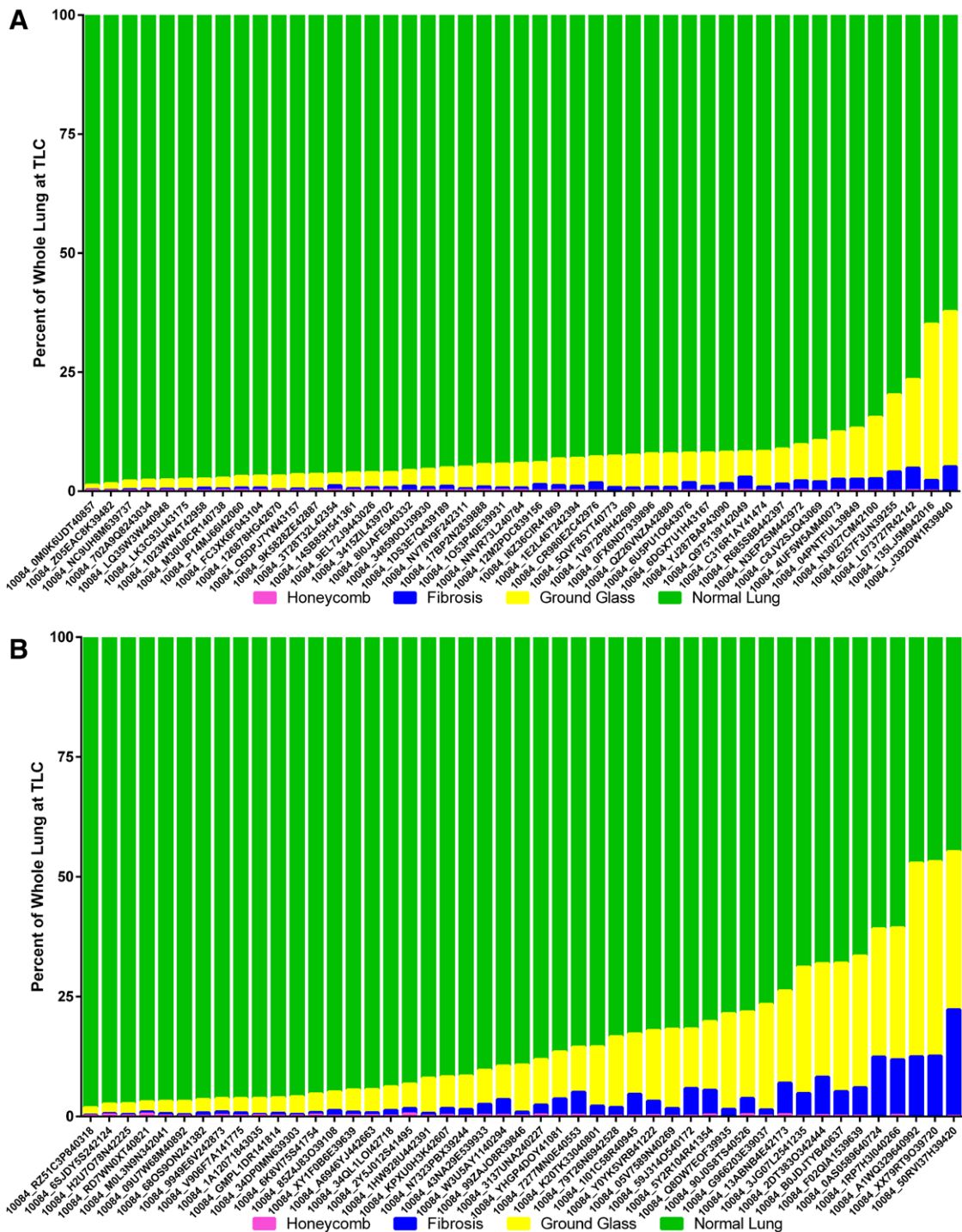


FIGURE 2. Quantitative image analysis for components of interstitial disease in no-CLAD controls (A) and CLAD cases (B). CLAD, chronic lung allograft dysfunction; TLC, total lung capacity.

undefined CLAD phenotypes. BOS cases also had lower scores for QLF than probable RAS or undefined CLAD phenotypes. In contrast, the extent of air-trapping was higher for BOS than with probable RAS or undefined CLAD phenotypes.

CLAD Phenotyping by HRCT Quantitative Image Analysis Scores

Given the potential misclassification of CLAD phenotypes in the absence of lung volumes, we explored CLAD

phenotype classification based solely on HRCT QIA at TLC (QILD) and RV (air-trapping). For CLAD cases, we plotted the proportion of lung with air-trapping versus the proportion with ILD (Figure 5). Based on the distribution of points on the graph, we established thresholds for abnormal QILD (>7.5%) and air-trapping (>10.0%), corresponding to 4 radiographic phenotypes. Seventeen CLAD cases had high QILD and low air-trapping scores and were classified as radiographic RAS. Thirteen had low QILD and high air-trapping scores and were classified as

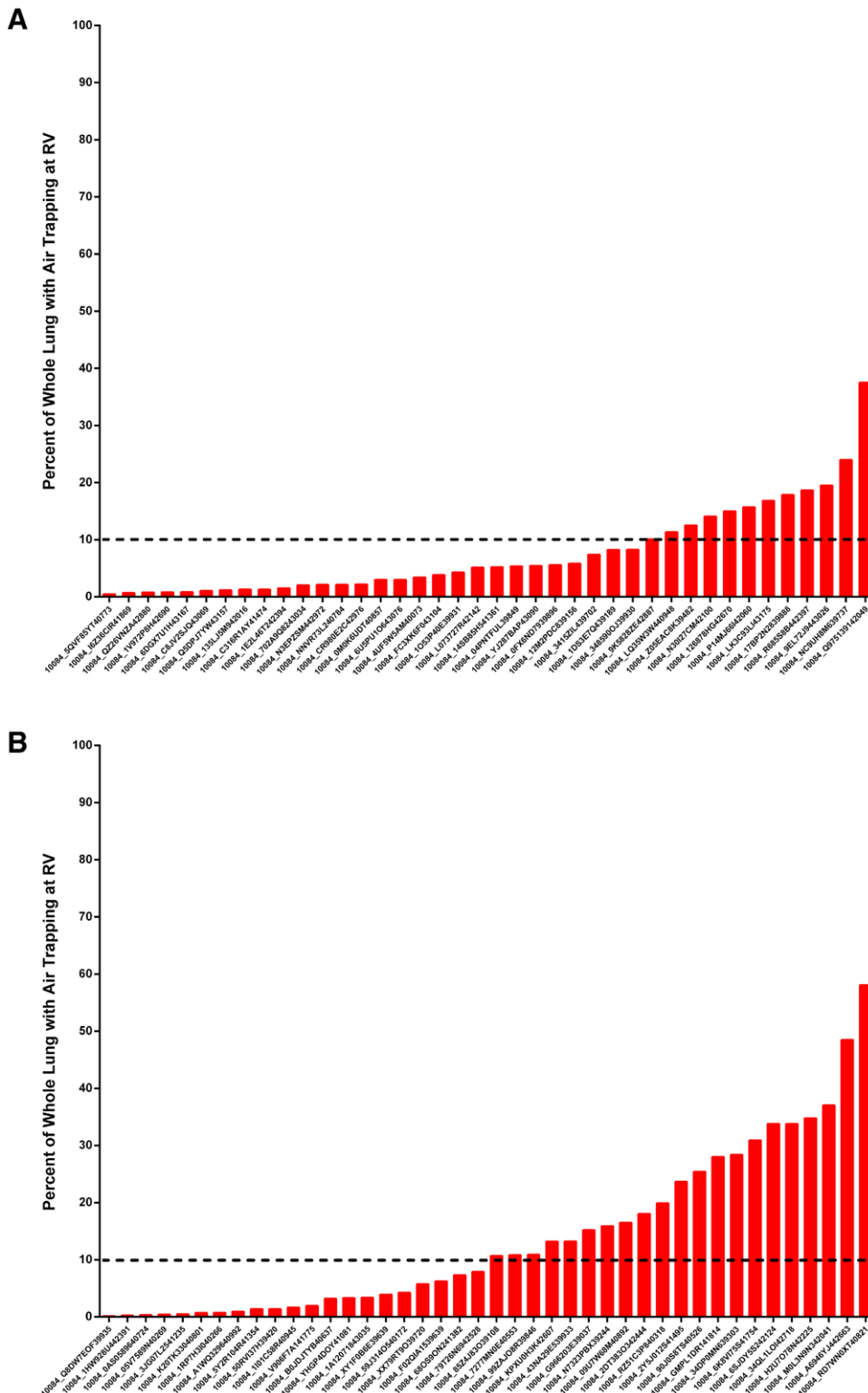


FIGURE 3. Quantitative image analysis for air-trapping in no-CLAD controls (A) and CLAD cases (B). CLAD, chronic lung allograft dysfunction; RV, residual volume.

radiographic BOS. Eight cases had high QILD and high air-trapping scores and were classified as mixed CLAD. Four cases had low scores for both were classified as undefined CLAD (Figure 5).

Agreement between 2019 ISHLT consensus and HRCT QIA CLAD phenotypes was 66.7% (28/42), with a corresponding Kappa of 0.550 (SE = 0.089, 95% confidence

interval, 0.375-0.725) indicating moderate agreement. There were 14 instances of discordant phenotype classification: 1 case defined as BOS by ISHLT consensus was classified as mixed by HRCT QIA; 2 cases of mixed CLAD by ISHLT consensus were classified as RAS by HRCT QIA; and 2 cases of probable RAS by ISHLT consensus was classified as mixed by HRCT QIA. Most CLAD cases

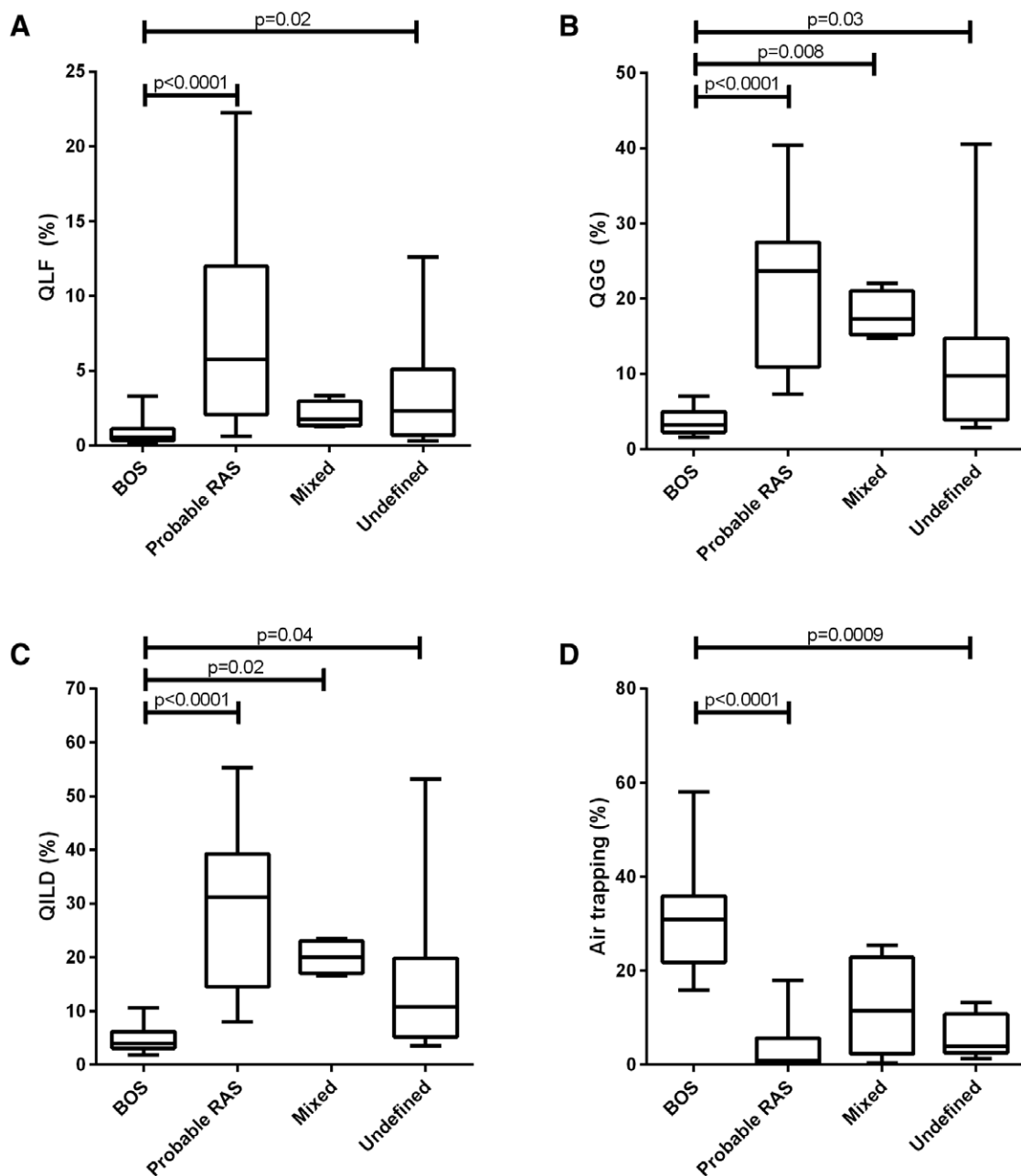


FIGURE 4. Box plots for chest HRCT QIA scores for each CLAD phenotype. *P* represents Dunn's multiple comparisons tests. BOS, bronchiolitis obliterans syndrome; CLAD, chronic lung allograft dysfunction; HRCT, high-resolution computed tomography; QGG, quantitation of ground glass; QIA, quantitative image analysis; QILD, quantitation of interstitial lung disease; RAS, restrictive allograft syndrome.

with an undefined 2019 ISHLT consensus phenotype were reclassified by HRCT QIA: 13 undefined cases with conventional classification and only 4 using QIA methods. Of the 9 undefined cases that were classified differently by CT quantification, 5 were reclassified as RAS, 1 as BOS, and 3 as mixed phenotype.

HRCT QIA-based CLAD Phenotyping Predicts Outcomes

The estimated post-CT survival for each CLAD phenotype, determined by conventional classification methods and by HRCT QIA is shown in Figure 6. With each classification method, survival was similarly worse for mixed disease and RAS, as compared with BOS. However, the cases classified as undefined based on conventional methods had survival most similar to those classified as BOS,

while those classified as undefined by CT quantification behaved as if they did not have CLAD. For QIA determined phenotypes, the relative risk of death after chest HRCT was higher for RAS, BOS, and mixed phenotypes as compared with no-CLAD controls (Table 3). Survival was also significantly worse for mixed CLAD than for BOS. While no mortality was observed in patients classified as undefined CLAD based on QIA, the sample size was too small for statistical comparisons.

We also examined phenotype changes over time based on conventional criteria. We did not observe any changes in phenotype for those with BOS or mixed phenotype at CLAD onset. However, 4 probable RAS patients were observed to change to a mixed phenotype during follow-up. At CLAD onset, QIA classified 2 of these cases as RAS and 2 as mixed phenotype. Among the undefined CLAD

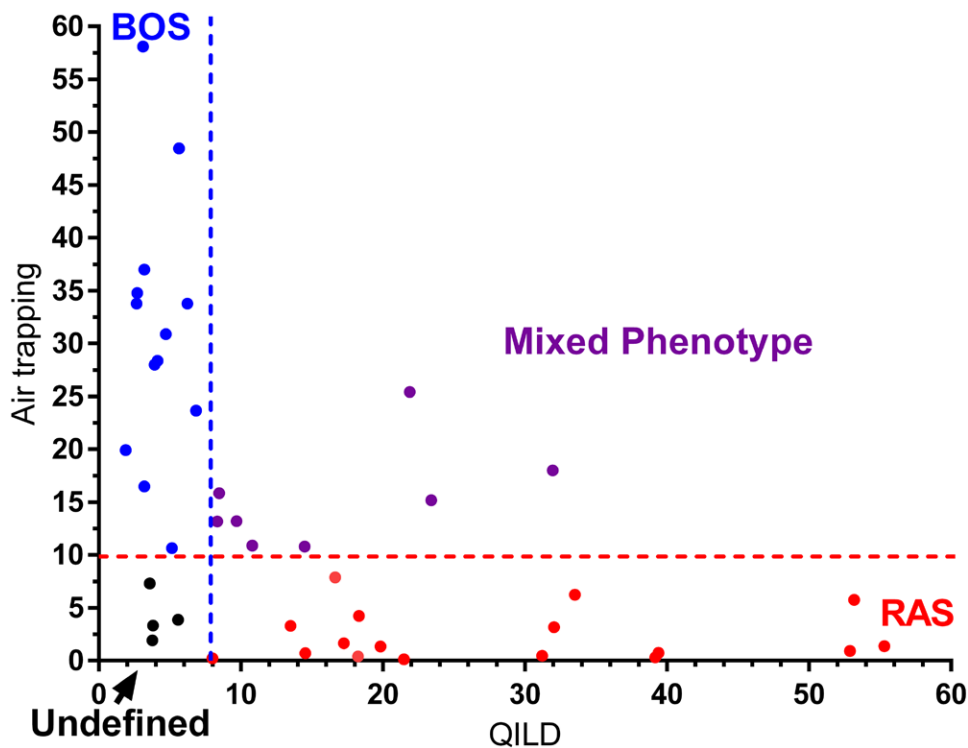


FIGURE 5. CLAD phenotypes were determined by quantitative image analysis for ILD (X axis) and air-trapping (Y axis). Thresholds for abnormal drawn at 7.5% for QILD and 10.0% for air-trapping. BOS phenotype is defined by high air-trapping and low QILD scores. RAS phenotype is defined by high QILD and low air-trapping scores. Mixed CLAD is defined as high scores for both, and undefined is defined as low scores for both. BOS, bronchiolitis obliterans syndrome; CLAD, chronic lung allograft dysfunction; QILD, quantitation of interstitial lung disease; RAS, restrictive allograft syndrome.

cases at CLAD onset, 2 cases eventually met criteria for BOS, one of which was classified as BOS by QIA at CLAD onset. Four undefined cases at CLAD onset developed probable RAS, 3 of which were classified as RAS and 1 as Mixed CLAD by QIA at CLAD onset. Finally, 2 undefined cases developed a mixed CLAD phenotype, both of which were classified as RAS at CLAD onset by QIA.

DISCUSSION

The development of CLAD is the most important limitation for long-term survival after lung transplantation. Although CLAD in general has a poor prognosis, CLAD phenotypes translate to meaningful differences in prognosis.^{2-5,8} It is also speculated that CLAD phenotypes could involve different molecular pathways and that the phenotype may ultimately guide treatment selection. In this article, we explored computer-aided quantification of interstitial disease and air-trapping in chest HRCT images at CLAD onset, and we demonstrate that chest HRCT QIA may provide useful phenotype data.

Our findings fit with expectations and provide construct validity for HRCT QIA measures at CLAD onset. There was moderate agreement, based on a Kappa statistic, between conventional and QIA phenotype classification methods. The implications of QIA determined phenotypes were also similar to conventional methods, in that survival was generally worse for mixed and RAS phenotypes, as compared with BOS. However, while cases classified as undefined phenotype based on conventional methods had observed outcomes most similar to those classified as BOS, those classified as undefined by QIA behaved as if they did not have CLAD. Given the small number ($n = 4$) of

undefined cases by QIA, it is not possible to make any firm conclusions, but it will be interesting to study this group further in larger cohorts.

Conventional CLAD phenotype classification relies on measurements of TLC at CLAD onset and on serial TLC measures before CLAD to establish the post-transplant baseline. Many lung transplant centers, including ours, do not perform routine TLC measurements post-transplant because of limitations in availability. A potential advantage of QIA is that it does not rely on prior TLC measures. The recent ISHLT consensus statement stipulates that FVC loss of $\geq 20\%$ from the post-transplant baseline can be used to imply restriction in the absence of TLC measures.^{6,7} However, FVC loss may also occur with air-trapping and hyperinflation, which are hallmarks of severe obstruction, and may result in misclassification. QIA-based phenotype classification also avoids the potential problems with inferring restriction from FVC loss.

In addition, our findings suggest that QIA could be a more sensitive classification method at CLAD onset. A relatively high proportion of CLAD cases were of undefined phenotype by conventional classification methods at CLAD onset. Most of these cases were classified as RAS or Mixed CLAD by QIA. This suggests that the FVC loss $\geq 20\%$ criteria may be insensitive for identifying restriction at CLAD onset. Furthermore, most undefined cases at CLAD onset eventually met conventional criteria for BOS, probable RAS, or mixed CLAD. Interestingly, for these cases where the phenotype became apparent during follow-up, QIA at CLAD onset often predicted the final phenotype. These findings raise the key question about whether QIA measures in patients with acute lung allograft

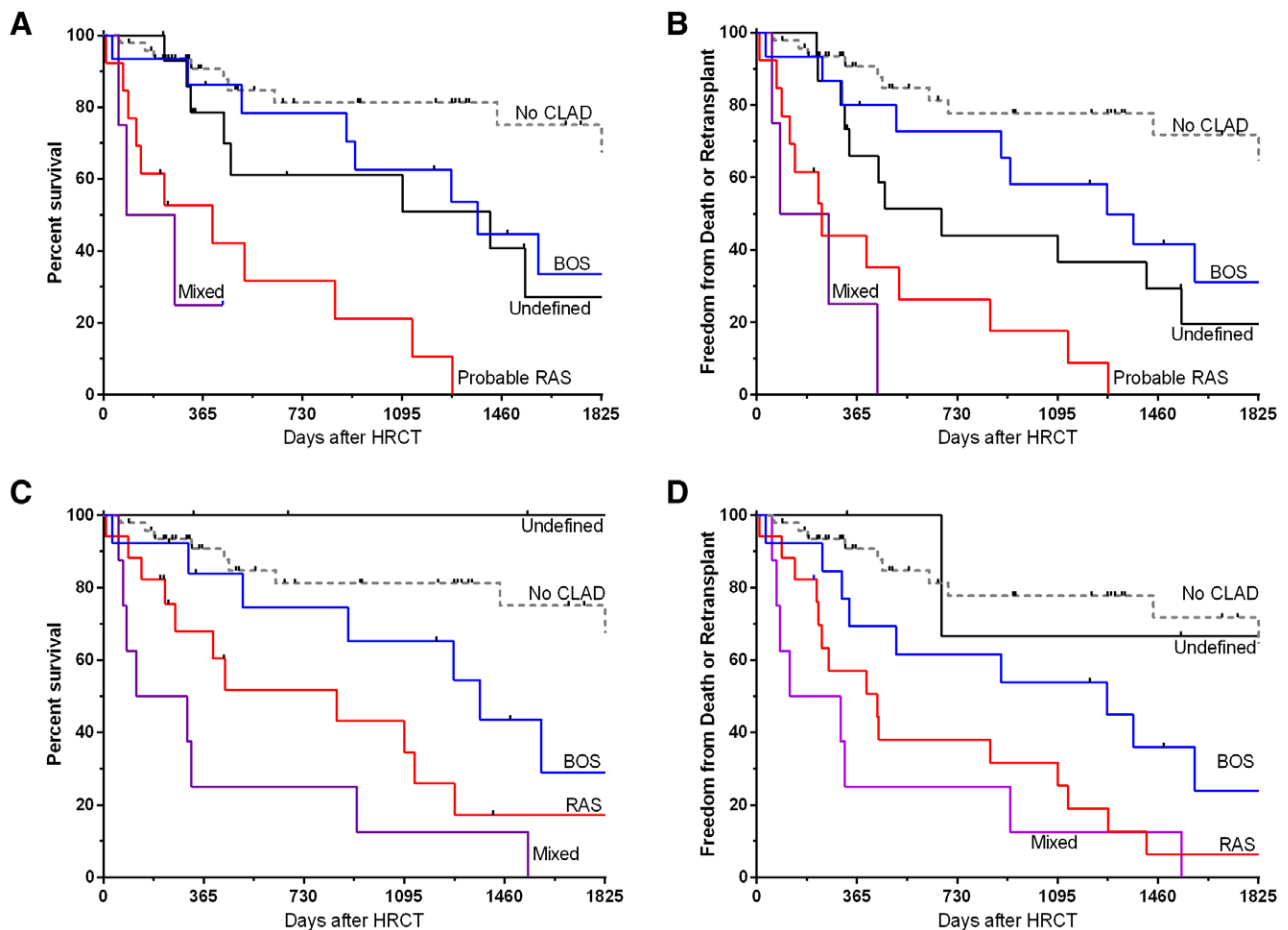


FIGURE 6. Kaplan-Meier curves for overall survival and freedom from death or retransplant by phenotype as determined by conventional classification (A and B) and by QIA-based classification (C and D). BOS, bronchiolitis obliterans syndrome; CLAD, chronic lung allograft dysfunction; HRCT, high-resolution computed tomography; QIA, quantitative image analysis; RAS, restrictive allograft syndrome.

dysfunction (FEV1 decline $\geq 10\%$ to $<20\%$) could predict progression to CLAD or the eventual CLAD phenotype. Future studies should be designed to address this question.

In a previous single-center retrospective study, a quantitative density metric (QDM) derived from HRCT histograms was associated with survival after CLAD onset.¹⁰ QDM values above the median were also associated with increased mortality within BOS and RAS subtypes. There are important differences between the HRCT histogram analyses in the previous study and our current methods for quantifying interstitial disease. We utilized a texture

feature classification that extends a simple density threshold approach for parenchymal assessment.^{12,13} In addition, we integrated measures of air trapping to further the ability to phenotype patients, which has not been done before. Thus like QDM, QILD scores predict worse survival, but with the addition of air-trapping scores patients can be phenotyped from a single HRCT examination analogous to the ISHLT consensus that includes mixed and undefined phenotypes, in addition to RAS and BOS.

Inherent with any retrospective design, there are important limitations to our study. As noted above, this study lacks TLC measurement as lung volumes are not routinely performed in our center. Our study is also limited by relatively small sample size, especially within subgroups. Validation in an independent cohort is required to draw firm conclusions about the accuracy or prognostic value. This is a single-center study and findings may not be generalizable. Although our standard of care HRCT protocol for lung transplant patients includes noncontrast images at end inspiration (TLC) and end expiration (RV), the rigor of ensuing standardized breath-holds is not confirmed. Although a goal of this study was to eliminate subjectivity in CLAD phenotype determination, the QIA measures used are not specific for CLAD parenchymal or airway abnormalities and can be confounded by other comorbid disease processes. We excluded cases with superimposed radiologic findings and this may limit the generalizability of our methods. Ideally, a chest CT would be repeated after

TABLE 3.

Cox proportional hazards model for survival after HRCT based on quantitative image analysis determined phenotype

Comparison		Risk ratio	P	Lower 95%	Upper 95%
Level 1	Level 2				
RAS	No-CLAD	6.27	<0.0001	2.57	15.28
BOS	No-CLAD	3.15	0.02	1.21	8.21
Mixed	No-CLAD	11.81	<0.0001	4.41	31.58
Mixed	BOS	3.75	0.01	1.38	10.17
Mixed	RAS	1.88	0.17	0.76	4.63
RAS	BOS	1.99	0.14	0.80	4.93

BOS, bronchiolitis obliterans syndrome; CLAD, chronic lung allograft dysfunction; RAS, restrictive allograft syndrome.

the resolution of the confounding condition, but in this retrospective study, we could not control when the CT was done or whether it was repeated. Additionally, the selection of thresholds to define CLAD phenotypes was somewhat arbitrary, and these thresholds require validation and potential optimization. We also included only bilateral lung transplant recipients to avoid the confounding effects introduced by a native lung. Finally, the QIA software we used to score HRCTs is not clinically available and it would not be possible to apply our methods in the clinical setting at this time. However, numerous clinical trials have utilized our QIA tool as secondary or exploratory endpoints.¹⁴⁻¹⁷ Future studies could potentially employ HRCT QIA at screening as eligibility criteria or as stratification within CLAD treatment arms of a clinical trial.

In this initial exploratory study, we demonstrate that computer-aided quantification of interstitial lung disease and air-trapping on chest HRCT at CLAD onset can effectively identify clinically relevant CLAD phenotypes with survival implications. More work is required to determine optimal cutoffs and to validate in external cohorts. However, chest HRCT QIA at CLAD onset appears promising as a method for precise determination of CLAD phenotypes and could be an important tool for CLAD research aimed at discovering new treatments and improving outcomes for lung transplant patients.

REFERENCES

1. DerHovanesian A, Wallace WD, Lynch JP III, et al. Chronic lung allograft dysfunction: evolving concepts and therapies. *Semin Respir Crit Care Med*. 2018;39:155–171.
2. DerHovanesian A, Todd JL, Zhang A, et al. Validation and refinement of chronic lung allograft dysfunction phenotypes in bilateral and single lung recipients. *Ann Am Thorac Soc*. 2016;13:627–635.
3. Sato M, Hwang DM, Waddell TK, et al. Progression pattern of restrictive allograft syndrome after lung transplantation. *J Heart Lung Transplant*. 2013;32:23–30.
4. Sato M, Waddell TK, Wagnetz U, et al. Restrictive allograft syndrome (RAS): a novel form of chronic lung allograft dysfunction. *J Heart Lung Transplant*. 2011;30:735–742.
5. Todd JL, Jain R, Pavlisko EN, et al. Impact of forced vital capacity loss on survival after the onset of chronic lung allograft dysfunction. *Am J Respir Crit Care Med*. 2014;189:159–166.
6. Glanville AR, Verleden GM, Todd JL, et al. Chronic lung allograft dysfunction: definition and update of restrictive allograft syndrome – a consensus report from the Pulmonary Council of the ISHLT. *J Heart Lung Transplant*. 2019;38:483–492.
7. Verleden GM, Glanville AR, Lease ED, et al. Chronic lung allograft dysfunction: definition, diagnostic criteria, and approaches to treatment – a consensus report from the Pulmonary Council of the ISHLT. *J Heart Lung Transplant*. 2019;38:493–503.
8. Levy L, Huszti E, Renaud-Picard B, et al. Risk assessment of chronic lung allograft dysfunction phenotypes: validation and proposed refinement of the 2019 International Society for Heart and Lung Transplantation classification system. *J Heart Lung Transplant*. 2020;39:761–770.
9. Arakawa H, Webb WR. Air trapping on expiratory high-resolution CT scans in the absence of inspiratory scan abnormalities: correlation with pulmonary function tests and differential diagnosis. *AJR Am J Roentgenol*. 1998;170:1349–1353.
10. Horie M, Salazar P, Saito T, et al. Quantitative chest CT for subtyping chronic lung allograft dysfunction and its association with survival. *Clin Transplant*. 2018;32:e13233.
11. Weigt SS, Copeland CAF, Derhovanessian A, et al. Colonization with small conidia *Aspergillus* species is associated with bronchiolitis obliterans syndrome: a two-center validation study. *Am J Transplant*. 2013;13:919–927.
12. Kim HG, Tashkin DP, Clements PJ, et al. A computer-aided diagnosis system for quantitative scoring of extent of lung fibrosis in scleroderma patients. *Clin Exp Rheumatol*. 2010;28:S26–S35.
13. Kim HJ, Li G, Gjertson D, et al. Classification of parenchymal abnormality in scleroderma lung using a novel approach to denoise images collected via a multicenter study. *Acad Radiol*. 2008;15:1004–1016.
14. Lancaster L, Goldin J, Trampisch M, et al. Effects of nintedanib on Quantitative Lung Fibrosis Score in idiopathic pulmonary fibrosis. *Open Respir Med J*. 2020;14:22–31.
15. Palmer SM, Snyder L, Todd JL, et al. Randomized, double-blind, placebo-controlled, phase 2 trial of BMS-986020, a lysophosphatidic acid receptor antagonist for the treatment of idiopathic pulmonary fibrosis. *Chest*. 2018;154:1061–1069.
16. Raghu G, Scholand MB, de Andrade J, et al. FG-3019 anti-connective tissue growth factor monoclonal antibody: results of an open-label clinical trial in idiopathic pulmonary fibrosis. *Eur Respir J*. 2016;47:1481–1491.
17. Richeldi L, Fernández Pérez ER, Costabel U, et al. Pamrevlumab, an anti-connective tissue growth factor therapy, for idiopathic pulmonary fibrosis (PRAISE): a phase 2, randomised, double-blind, placebo-controlled trial. *Lancet Respir Med*. 2020;8:25–33.